UNVEILING "*THE SCREAM*" BY EDVARD MUNCH: ITERATIVE FUZZY C-MEANS ANALYSIS OF MACRO-XRF MAPPING

M.L. Cardinali [1], F. Albertin [2], L. Cartechini [2*], I. C. A. Sandu [3], E. Storevik Tveit [3], A. Romani [2,4], C. Grazia [2,4], R. P. de Freitas [2,5], V. Bruni [1,6], D. Vitulano [1,6], F. Rosi [2]*

[1] Department of Basic and Applied Sciences for Engineering, Sapienza Rome University, Rome, Italy;
[2] Istituto di Scienze e Tecnologie Chimiche "Giulio Natta" SCITEC – CNR, Perugia, Italy;
[3] Paintings Conservation Section, Department of Collection Care and Management, MUNCH, Oslo, Norway;
[4] Centre of Excellence SMAArt and Department of Chemistry, Biology and Biotechnology, University of Perugia, Italy;
[5] Laboratory Federal Institute of Rio de Janeiro, Paracambi (RJ), Brazil;
[6] Istituto per le Applicazioni del Calcolo, IAC – CNR, Rome, Italy;

*Corresponding authors

ABSTRACT

"*The Scream*" by Edvard Munch belonging to the Munch Museum in Oslo has been analyzed using Macro X-ray Fluorescence (MA-XRF). The non-invasive imaging technique unveiled the elemental distribution of the inorganic materials of the painting and brought to light the artist's palette. The semi-unsupervised classification of MA-XRF datacube through an iterative Fuzzy C-Means (FCM)-based analysis was applied to shed light on the complex pigment mixture and execution technique used to create the iconic representation of "*The Scream*".
The analysis revealed the relationship between the main pigments and some other distinctive pigments characterized by low XRF intensities, such as cadmium yellows and oranges. The combination of a well-known investigating technique, such as MA-XRF, with the use of advanced algorithms, provided new informative chemical images representing Munch's painting technique.

***Index Terms*—** Hyperspectral XRF datacube, FCM, iterative clustering, painting technique.

1. INTRODUCTION

"*The Scream*" by Edvard Munch is indubitably one of the most celebrated modern paintings. The iconic symbol of human desolation has been created by the Norwegian artist in different versions, nowadays in different locations in Norway and USA [1]. This paper analyzes the painted version (83.5x66 cm^2, tempera and oil on unprepared cardboard) dated c. 1910? conserved at the Munch Museum in Oslo. This version of "*The Scream*" is characterized by a complex mixture of paints with variable thickness and shades, from the distinctive thick and intense red-orange nuances of the sky and the deep blue and green shadings of the background to the thin and cold tones of the central figure [2]. The painting was stolen in 2004 and on its return in 2006 the suffered damage was evident, especially in its lower-right corner as a discolored area. [1] Previous invasive investigations on some samples revealed both multiple layering and the wet-on-wet technique, consisting of the application of successive paints before the first layers have dried [2].
In the frame of a core project of the Munch Museum aimed at providing new scientific knowledge of Munch's paintings, scientific analyses of "*The Scream*" (1910?) were performed within a MOLAB analytical campaign in 2017 [3]. Integrated non-invasive investigations have been performed *in situ*, including imaging elemental and molecular techniques (MA-XRF and Hyperspectral Imaging HSI, preliminary results presented in [4, 5]). Detailed analyses on micro-samples of Cd pigments with synchrotron radiation-based X-ray micro-spectroscopy have been also published [6].
To achieve the goal of a better comprehension of this masterpiece and starting from this previous knowledge, MA-XRF data have been here examined. The technique enables the characterization of the elemental composition of the inorganic pigments/materials used by the artist and the scansion of the complete painting surface provides elemental maps which give researchers and restorers a comprehensive view and distribution of the constituent materials of the artwork [7-12].
Nevertheless, a deep study on the use of the different pigments, their mixtures, and the manifold paint layering of this complex painting, needs more complex computational approaches to explore and extract information from the high dimensional MA-XRF datacube.

Common procedures for hyperspectral data processing include dimensionality reduction methods [13-17] such as principal components analysis (PCA), independent component analysis (ICA), non-negative matrix factorization (NMF), or features extraction methods, and spectral unmixing [18, 19]. The former class is often necessary for identifying and eliminating statistical redundancies of hyperspectral data while keeping as much spectral information as possible; the latter is applied to solve the mixture problem, i.e., to separate the spectral components at each pixel, requiring the estimation of pure spectral endmembers and the mixing function. When used for classification purposes, both often suffer from the fact that most relevant pigments are emphasized, while neglecting those less representative *(low concentration)* or characterized by less efficient detection.

To overcome this problem, unsupervised clustering methods can be used to identify those pixels having the same spectral composition [20]. To further refine the analysis, in this paper a Fuzzy C-Means (FCM) clustering method is applied in an iterative and nonlinear fashion. After each FCM phase, the dominating signal is eliminated to better classify the remaining spectral contribution. In this way, separate and successive analyses of points having the same spectral composition contribute to further emphasizing element separation, resulting in more informative chemical images.

2. EXPERIMENTAL DATA

MA-XRF data were obtained *via* analysis performed *in situ* using the CRONO scanner by XGLab (Bruker Nano Analytics). The measurement head of the system, equipped with a large area silicon drift detector and an Rh anode tube, is mounted on a motorized XYZ stage to perform large-area scanning (450 mm by 600 mm and 75 mm for focusing axis).

The painting was analyzed using 50 kV and 200 µA, a 1-mm pinhole collimator, a linear speed of 20 mm/s, and an acquisition time of 40 ms per point/spectrum [6]. Due to the instrument's set-up and the object dimension, the acquisition of the entire surface was achieved in four data-taking sessions and the datacubes were successively merged.

The complete map results of 835 x 675 pixels/spectra and the data were binned from 4096 to 2048 channels to improve the signal-to-noise ratio.

The first analyses of the data cube were performed using PyMCA and DataMuncher software: the raw spectral data have been calibrated, fitted, and the spectral intervals of specific element peaks have been mapped and imaged.

3. METHODS

To promote the separation of painting pigments, an iterative clustering method was used. The aim was to emphasize regions in the painting having similar paint compositions and to apply components separation in each class independently. The Fuzzy C-Means (FCM) clustering method [21] was chosen to process the MAXRF datacube and generate compositional images of the painting. FCM is a well-known unsupervised fuzzy clustering technique based on the minimization of an objective function. When applied in the context of spectral images, it allows for both identifying structures in the data and segmenting the image into regions with similar spectral properties. Once the number of required classes has been set, FCM assigns to each pixel a degree of membership for every class; the iteration stops when either the maximum number of iterations is reached, or the variation of the objective function is less than a predefined threshold. The resulting soft partitioning is then converted to a hard partitioning according to a maximum membership rule.

In the present study, a blind FCM was combined with a supervised approach. Based on FCM classification, classes representing areas where a certain element is prominent were identified; those classes were then investigated by iteratively removing peaks associated with dominant elements and performing FCM. The process stops when no more elements could be found or FCM was no longer able to distinguish classes.

The basic steps of the proposed two-stage analysis are given as follows:

First stage: initial guess

1. Partition data using FCM and let $C_i, i = 1, \dots, n$, be the identified classes
2. Identify classes of interest by looking at their central spectrum and group them according to their dominant peaks - classes sharing the same dominant element are assigned to the same group. Let $G_j, j = 1, \dots, K$,, be the identified groups.

Second stage: iterative process

3. For each group $G_j, j = 1, \dots, k$ and for each class C_i in the group, proceed as it follows.
   While a predominant element can be detected and FCM separates classes in C_i:
   3.1 Remove peaks of predominant element from the spectra of pixels in C_i;
   3.2 Perform FCM on C_i.

Due to the small number of pixels in each class C_i and the reduced variability among them, at each iteration a merging operation based on the distance between the centers of the classes was performed on the FCM classification (3.2).

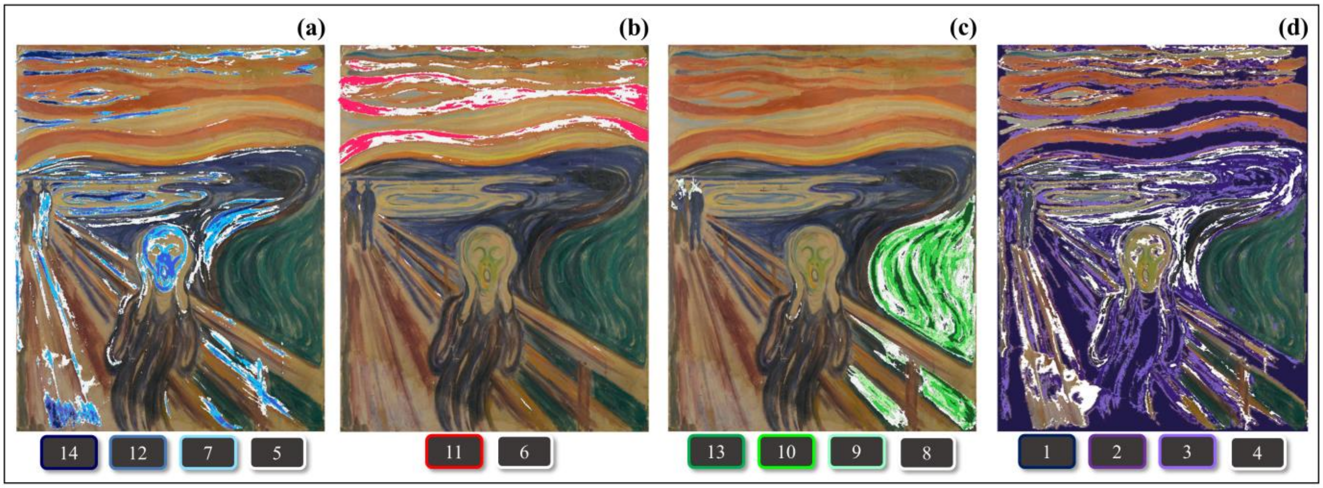

Figure 1: The main pigments that characterize the painting are retrieved in the first stage of the FCM-based analysis: (a) zinc – for the lighter areas (classes 14,12,7,5), (b) mercury – for the red paints (classes 11 and 6), and (c) chrome – for the green zones (classes 13,10,9,8). Classes 1,2,3,4 (d) represent areas with a low XRF signal - light elements or a low paint thickness.

A moving average was applied to the input data to reduce noise. To preserve the spectral resolution, 4 and 8 channels moving average filters have been used before and after 8 keV (first 380 channels), respectively. It is worth observing that the proposed iterative procedure may be seen as a sort of two-layer neural network, where each FCM block resembles a one-layer network followed by a nonlinear operator.

4. RESULTS

To understand pigment distribution, a preliminary analysis of the MA-XRF datacube has been performed and elemental maps have been created. Indeed, since in general each pigment is characterized by a specific element, mapping elements in most cases means mapping a pigment (or a class of pigment).

MA-XRF reveals the following principal elements: K, Ca, Ba, Cr, Fe, Co, Zn, Cd, Hg, and Pb. Detected Ca, Ba and Fe signals are largely related to cardboard impurity. Zn, mainly used for the white and lighter colors, is present almost in all areas as pure (from the XRF point of view) pigment (ZnO) or as a mixture. Cr characterizes the green hues of the painting while Co was found in the blue shades. Cd, Hg, and Pb present a more complex distribution. Cd-based pigments were found in the red, orange, and yellow hues of the sky, and to create the main character's face shades, as investigated by [6]. The deeper red hues of the sky were created using vermillion (HgS) and Pb, most probably as minium (Pb_3O_4), as assessed by [2].

In most of the areas, especially in the sky, the overlapping of the distribution maps due to the mixture of colors and the manifold layering of the different brushstrokes make the elemental maps complex to be read. To promote the separation of spectra, thus highlighting compositional differences, blind FCM combined with a supervised analysis has been adopted through iterative and nonlinear processing of the datacube, as described in Section 3.

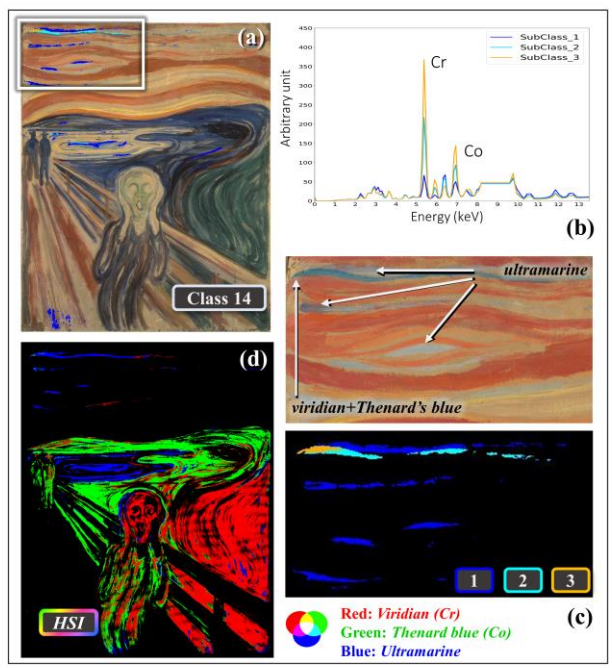

Figure 2: Visible image of the painting with sub-classification of class 14 (intense signal of Zn), obtained in the second stage of the FCM-based analysis (a). Spectra of the centre of the sub-classes showing the contribution of Cr and Co (b), detail of the sky with the 1-3 sub-classes distributions (c) pigment distribution by HSI (d).

A standard setting for the FCM parameters has been chosen. Taking into account the quantity of elements expected to be present on the basis of the previous analyses, 15 classes have been used as FCM input at step 1; it has been verified

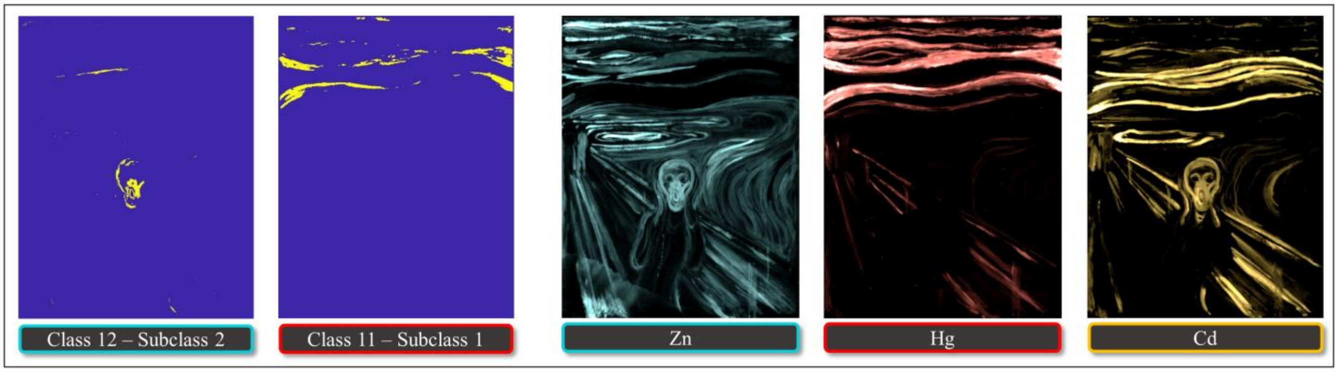

Figure 3: FCM classes weighting also by Cd: sub-class 2 of class 12 (dominated by Zn) and sub-class 1 of class 11 (dominated by Hg). These distributions and the comparison with elemental maps of Zn, Hg, and Cd revealed the correlation of Cd with Zn and Cr for the creation of the visage shades and the Cd with Hg for some dark red areas of the sky.

that choosing a greater number of classes and then adding a merging operation like the one performed in (3.2) would have led to comparable results.

The joint data clustering and hierarchical analysis of the central spectra of classes in the first stage of the FCM-based analysis split the data into four main groups – as shown in Figure 1. Classes 14, 12, 7, and 5 represent the distribution of Zn with the contribution of less intense signals of Co, Cr, Hg, Pb, and Cd (Figure 1a). The second group, which includes classes 11 and 6, is dominated by Hg with the contribution of lower signals of Zn, Pb, and Cd, and delineates the vermillion (HgS) distribution (Figure 1b). The third, composed of classes 13, 10, 9, and 8, is dominated by Cr with the contribution of Zn and describes the Cr-based pigment distribution mixed with ZnO to obtain the different hues (Figure 1c). Lastly, the group of classes 1-4 (Figure 1d) delineates painting areas where the XRF signal is low due to pigments composed of light elements, to a low amount of pigments, and/or to the contribution of the support – where cardboard was left exposed as part of the composition, according to "*a risparmio*" technique. The analysis of the spectra of the center of the classes of groups 1-3 highlights that classification is driven by the magnitude of the main peaks (Zn, Hg, and Cr respectively), and classes identify a decreasing of the principal element, thus visualizing regions made of a less pure pigment, since in mixture, or thinner painting layers.

To better investigate these results, the classes belonging to groups 1-3 have been further sub-divided by iteratively removing peaks associated with dominant elements (Zn, Hg, and Cr respectively) and performing again FCM in the *second stage* of the FCM-based analysis described in Section 3. The aim of this further sub-classification was to highlight and clarify any possible relationship between the principal and the less representative pigments.

The second stage of FCM-based analysis finds three subclasses for Class 14 (Figure 2a), which is dominated by the highest signal of Zn. The first one does not present prevalent peaks – except Zn (Figure 2b). The absence of other elements may suggest brushstrokes of "pure" Zn pigment. However, the distribution follows portions of the painting appearing in blue colors, such as the center of the lake and some lines of the sky (Figure 2c), due to the use of ultramarine blue (transparent to X-rays) as identified by HSI (Figure 2d) (details of the acquisition set-up in [6]). The second and the third classes present an increased amount of Co and Cr, and the integration with HSI results leads to identifying ZnO with viridian (Cr_2O_3 $2H_2O$) and Thénard's blue ($CoOAl_2O_3$) to create some of the dark blue brushstrokes in the sky. The overlay of subclasses 1-3 (Figure 2c) enables visualizing the creative process carried out by distinct brushstrokes or the use of the wet-wet technique for obtaining the various shades of this portion of the sky.

Despite the importance of Cd, the element that characterizes all orange and yellow shades of the painting, its distribution is not well represented by unsupervised FCM classification due to its low signal intensity (compared to other elements such as Zn) and by its ubiquitous use. The iterative and nonlinear clustering procedure allowed emphasizing the sub-classes characterized and weighted also by Cd. Figure 3 shows sub-class 2 of Class 12 – dominated by Zn –and sub-class 1 of class 11 – dominated by Hg, both weighted also by Cd. The first sub-class identifies Cd, Cr (and Zn) as elements to create the shades of the visage of the main character, created with CdS, viridian, and ZnO. The second reveals CdS-based brushstrokes in the deep red-orange hues of the sky, not visible in the Cd map since hidden by the strong signals of Hg. Unfortunately, the role of Pb and its association with other elements was not pointed out by this analysis, most probably due to its not predominance and its almost omnipresent co-presence with Hg.

5. CONCLUSIONS AND FUTURE PERSPECTIVE

The use of an iterative and nonlinear FCM-based analysis of MA-XRF datacube highlights important details of the complex painting technique of "*The Scream*" by E. Munch helping to clarify the complex paint mixtures and the relations among the main pigments. The first stage of the FCM-based analysis has led to classifying the element distributions into four main groups, three dominated by Zn, Hg, and Cr and their corresponding variation in intensity, one delineating painting areas with light elements, thin brushstrokes, and/or contribution of the support. The second stage of the analysis revealed the combination and distribution of pigments used to create peculiar shades. This is the case of ZnO and ultramarine, viridian, and Thénard's blue paints in the sky and the Cd-pigments used for the face of the principal character and for the deep red-orange regions of the sky. FCM technique turned out to be really effective in highlighting the distribution of the main pigments and, in some cases, their correlation with minor elements, making the double-level approach promising.

The proposed procedure requires further refinement to strengthen the capability of emphasizing the relationship between non-predominant elements.

Future research will be devoted to improving the two-stage FCM-based analysis by using more appropriate similarity metrics or nonlinear operators and employing a soft clustering approach, making it more sensitive to subtle differences in spectral distributions.

6. ACKNOWLEDGMENTS

The research was supported by the EU research project IPERION-CH (H2020-INFRAIA-2014-2015, n.654028) and by the Italian PNIR-SHINE "Rafforzamento del capitale umano delle Infrastrutture di Ricerca in attuazione del Piano Stralcio Ricerca e Innovazione 2015-2017".

7. REFERENCES

[1] T. Froysaker, N. Streeton et al., Public Paintings by Edvard Munch and His Contemporaries: Change and Conservation Challenges, Archetype Publications Ltd, London, 2015.

[2] B. Singer, T.E. Aslaksby et al., "Investigation of Materials Used by Edvard Munch", Studies in Conservation, 55(4), pp 274–292, 2010.

[3] B.G. Brunetti, C. Miliani et al., "Non-invasive investigations of paintings by portable instrumentation: the MOLAB experience", Topics in Current Chemistry, vol. 374, pp 1-35, 2016.

[4] I.C.A. Sandu, T. Ford et al., "The "Scream" by Edvard Munch - same motif, different colours, different techniques and approaches – a novel non-invasive comparative study of two of its versions", CHEM CH conference 2018, Bucharest.

[5] L. Cartechini, I.C.A. Sandu et al., "The "Scream" by Edvard Munch (1910): non-invasive integrated spectroscopic investigations of the painting materials", Ma-XRF Conference, Catania, 2019.

[6] L. Monico, L. Cartechini et al.,"Probing the chemistry of CdS paints in The Scream by *in situ* noninvasive spectroscopies and synchrotron radiation X-ray techniques", Science Advances, vol. 6, no. 20, 2020.

[7] M. Alfeld, W. De Nolf et. al., "Revealing hidden paint layers in oil paintings by means of scanning macro-XRF: a mock-up study based on Rembrandt's 'An old man in military costume", J. Anal. At. Spectrom., vol. 28, no. 1., pp. 40–51, 2013.

[8] S. De Meyer, F. Vanmeert et al., "Macroscopic x-ray powder diffraction imaging reveals Vermeer's discriminating use of lead white pigments in Girl with a Pearl Earring", Science Advances, vol. 5, no. 8, 2019

[9] F. Albertin, C. Ruberto et al., "'Ecce Homo' by Antonello da Messina, from non-invasive investigations to data fusion and dissemination", Scientific Reports, vol. 11, no. 1., 2021.

[10] D. Thurrowgood, D. Paterson et al., "A Hidden Portrait by Edgar Degas", Scientific Reports, vol. 6, no. 1, 2016.

[11] C. Ruberto, A. Mazzinghi et al., "Imaging study of Raffaello's 'La Muta' by a portable XRF spectrometer", Microchemical Journal, vol. 126. pp. 63–69, 2016.

[12] J. K. Delaney, K. A. Dooley et al., "Macroscale multimodal imaging reveals ancient painting production technology and the vogue in Greco-Roman Egypt", Scientific Reports, vol. 7, no.1, 2017.

[13] C. Sorzano, J. Vargas and A. Montano, "A survey of dimensionality reduction techniques", 2014.

[14] V. Bruni, M.L. Cardinali and D. Vitulano, "A Short Review on Minimum Description Length: An Application to Dimension Reduction in PCA", Entropy, 24(2):269, 2022.

[15] M. Alfeld, M. Wahabzada et al., "Non-negative factor analysis supporting the interpretation of elemental distribution images acquired by XRF Non-negative factor analysis supporting the interpretation of elemental distribution images acquired by XRF", Journal of Physics Conference Series, 499, 012013, 2014.

[16] G. Magkanas, H. Bagán et al., "Illuminated manuscript analysis methodology using MA-XRF and NMF: Application on the Liber Feudorum Maior", Microchemical Journal, vol. 165, 106112, 2021.

[17] H. Santos, C. Caliri et al., "Identification of forgeries in historical enamels by combining the non-destructive scanning XRF imaging and alpha-PIXE portable techniques", Microchemical Journal, vol. 124, pp 241-246, 2015.

[18] N. Keshava, J.F. Mustard, "Spectral Unmixing", IEEE Signal Processing Magazine 19, no. 1, pp 44–57. 2002.

[19] H. Deborah, M.O. Ulfarsson and J. Sigurdsson, "Fully Constrained Least Squares Linear Spectral Unmixing of The Scream (Verso, 1893)", IEEE WHISPERS workshop, 2021.

[20] S. Kogou, L. Lee et al., "A new approach to the interpretation of XRF spectral imaging data using neural networks", X-Ray Spectrom, 50, pp 310–319, 2021.

[21] J.C. Bezdek, "Pattern Recognition with Fuzzy Objective Function Algorithms", Plenum Press, New York, 1981.